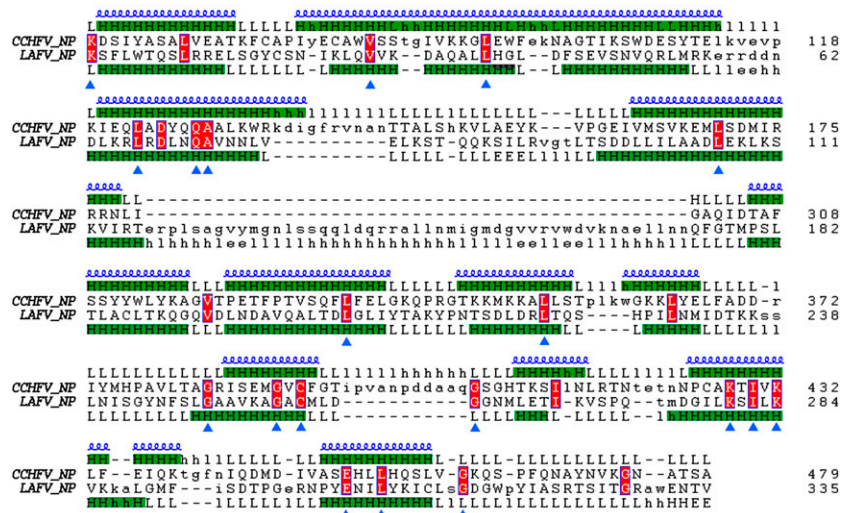
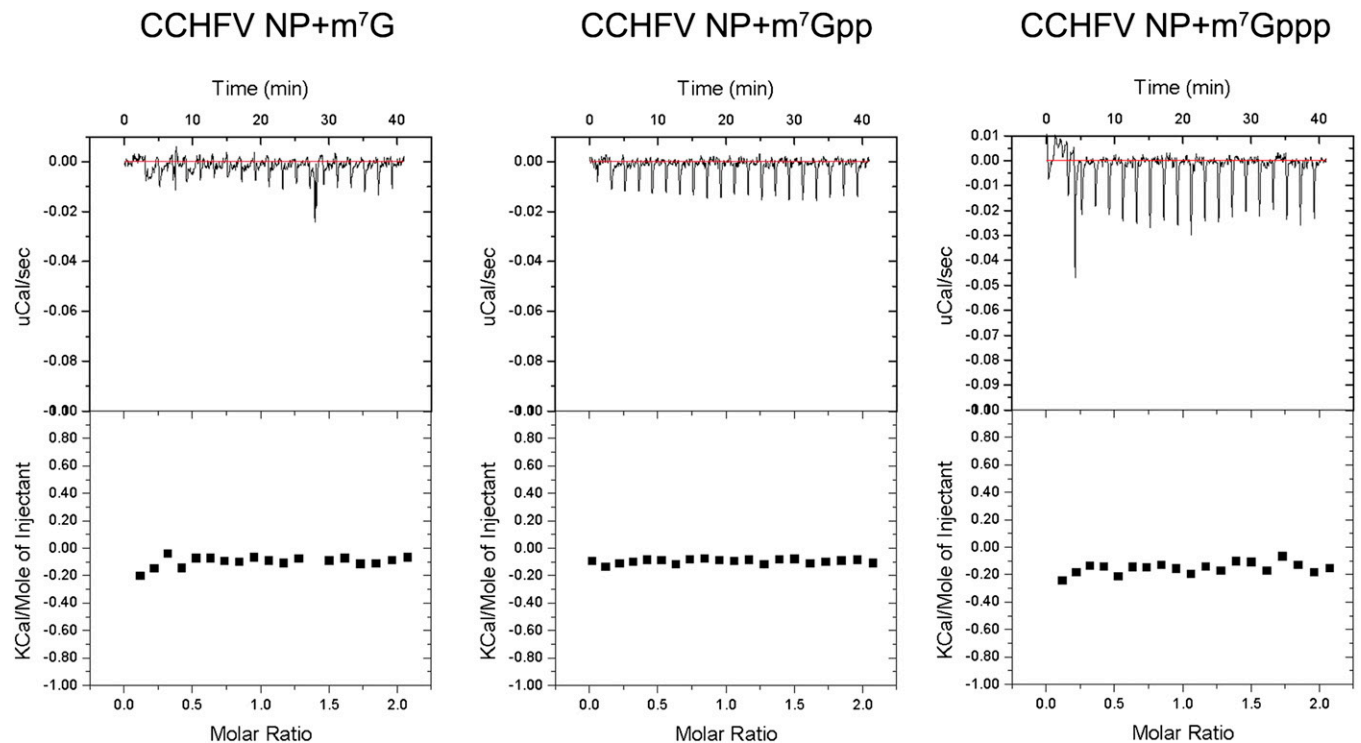


# Supporting Information

Guo et al. 10.1073/pnas.1200808109



**Fig. S1.** Sequence alignment between the Crimean–Congo hemorrhagic fever virus (CCHFV) nucleoprotein (NP) head domain and the Lassa fever virus (LASV) NP N-terminal domain. DALI analysis of the major component of the CCHFV NP head domain (residues 59–180 and 300–479) showed its similarity with the N-terminal domain of LASV NP (Protein Data Bank, PDB code: 3MX5, Z score = 15.5, rmsd value of 3.2 Å for a total of 259 aligned residues). Identical residues in the primary sequence are shown in white on a red background. Residues that overlap in space are indicated with a blue triangle underneath. The observed  $\alpha$  helices are labeled green and indicated above the alignment.



**Fig. S2.** Binding affinities of cap analogs. Binding affinities of cap analogs, i.e.,  $m^7G$ ,  $m^7Gpp$ ,  $m^7Gppp$  to wild-type CCHFV NP was measured by isothermal titration calorimetry (ITC). The binding of cap analogs to wild-type CCHFV NP at a concentration of 0.1 mM was determined with ITC by stepwise injection of each compound in a 0.3-mM solution (Sigma-Aldrich), using a VP-ITC microcalorimeter (MicroCal). ITC data were collected at 25 °C and analyzed using ORIGIN (MicroCal).

CCHFV NP:RNA molar ratio

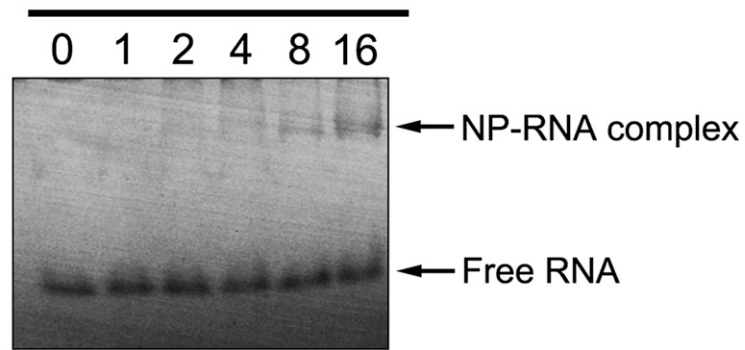


**Fig. S3.** EMSA of CCHFV with 24-nt ssRNA. The interaction of recombinant CCHFV NP with a 24-nt poly(rA) probe was tested by electrophoretic mobility shift assay according to standard protocol. The reaction buffer was 20 mM Hepes pH 7.0, 200 mM NaCl. The concentration of RNA was kept constant at 6.5  $\mu$ M; protein and RNA sample were incubated in 37  $^{\circ}$ C for 30 min. Free RNA and the NP-RNA complex were separated on a nondenaturing 10% (wt/vol) polyacrylamide gel and stained with ethidium bromide.

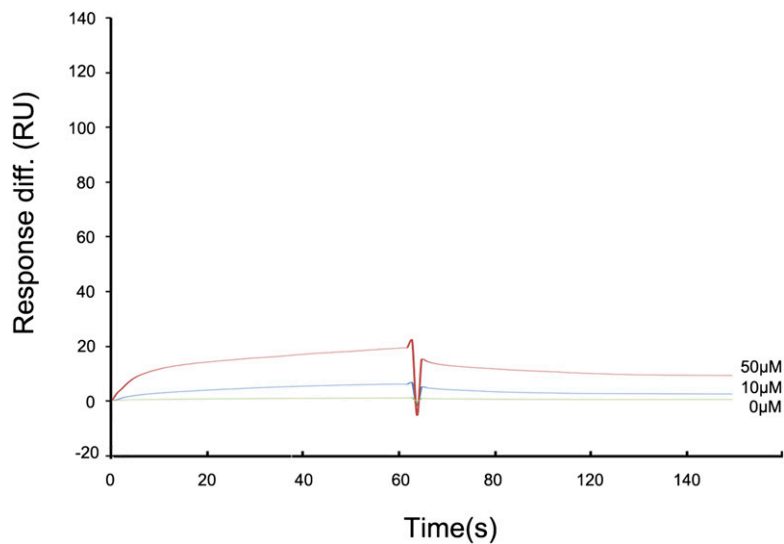


**Fig. S4.** Sensorgram of binding of wild-type CCHFV NP to immobilized RNA. A biotinylated 2'-O-methylated RNA oligonucleotide with the sequence 5' UUU UUU UUU UUU UUU UU 3' was immobilized on an SA sensor chip (GE Health). Surface plasmon resonance measurements were carried out with a BIAcore 3000 (GE Health) at 25  $^{\circ}$ C, using different concentrations of purified wild-type CCHFV NP. The curve was drawn from the average of two independent assays. The resonance unit (RU) value shows extremely low binding affinity even at a protein concentration as high as 50  $\mu$ M.

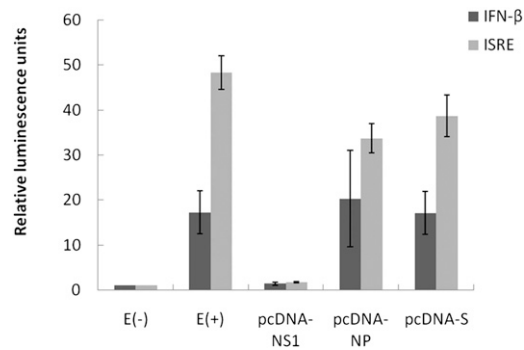


**Fig. 55.** Sendai virus-induced activation of the IFN- $\beta$  and IFN-stimulated response element (ISRE) promoters shows that CCHFV NP has no effect on type I IFN response. The full-length CCHFV 5 segment (strain YL04057), the ORF of CCHFV nucleoprotein NP, and the ORF of influenza A virus PR8 NS1 (control) were cloned into pcDNA3.1(+) vectors (Invitrogen), giving mammalian expression vectors pcDNA-S, pcDNA-NP, and pcDNA-NS1, respectively. HEK 293T cells ( $5 \times 10^4$  per well) were cotransfected with the reporter plasmids pGL3-IFN- $\beta$  or pGL3-ISRE, pRL-TK, and the mammalian expression vectors pcDNA-S, pcDNA-NP, or pcDNA-NS1. Twenty-four hours after transfection, cells were infected with Sendai virus for 12 h before assaying luminescence activity. Values displayed reflect relative luminescence units corrected to an uninfected, empty vector control. E(-) and E(+) indicate an uninfected empty vector control and an infected empty vector control, respectively.

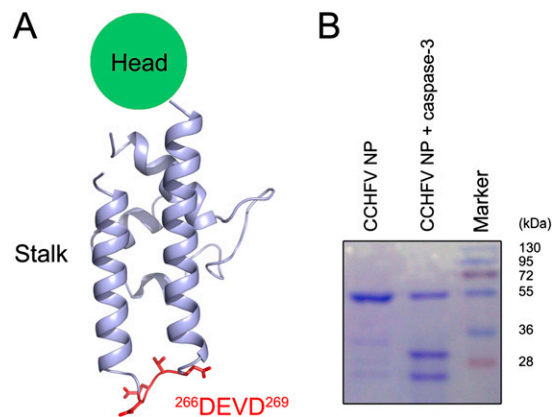


**Fig. 56.** Caspase-3 proteolysis of CCHFV NP in vitro. (A) Cleavage site,  $^{266}\text{DEVD}^{269}$ , is shown in stick representation in red. (B) Proteolytic activity of caspase-3 on CCHFV NP was checked by SDS/PAGE.

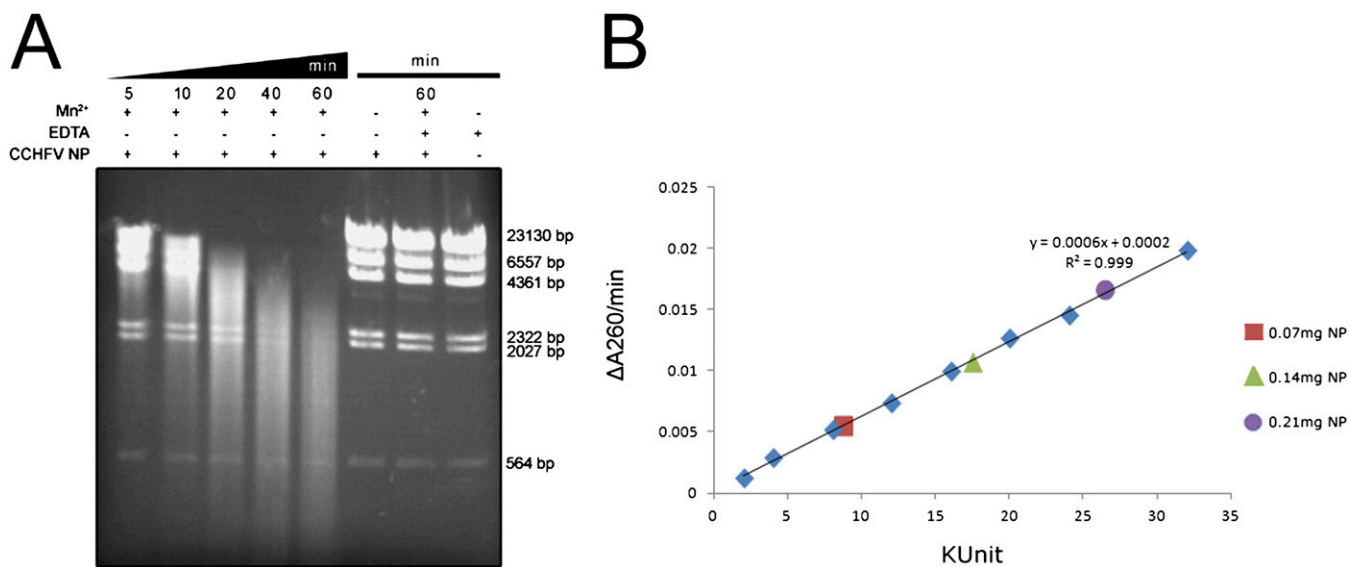


**Fig. S7.** (A) CCHFV degrades long-structured dsDNA in vitro in the presence of Mn<sup>2+</sup>. Time series for the in vitro degradation of long and highly structured dsDNA ( $\lambda$ -DNA) is shown. Products of 0.3  $\mu$ M purified CCHFV NP, reacted with a 100 ng/ $\mu$ l  $\lambda$ -DNA substrate at 37 °C, are shown after 5, 10, 20, 40, and 60 min. Reaction products were loaded onto a 1.5% (wt/vol) agarose gel and stained with ethidium bromide. (B) Measurement of the specific activity of CCHFV NP. Buffer contained 20 mM HEPES, pH 6.8, 100 mM NaCl, and 5 mM MnCl<sub>2</sub>. A total of 200  $\mu$ g/mL calf thymus DNA (purchased from Sigma) was used as a substrate for the reaction at 37 °C, and DNase I at various concentrations was used as a control for calibrating a standard curve. CCHFV NP was then tested independently at three different concentrations, giving a DNA endonuclease specific activity of  $1.3 \times 10^5$  units/mg.

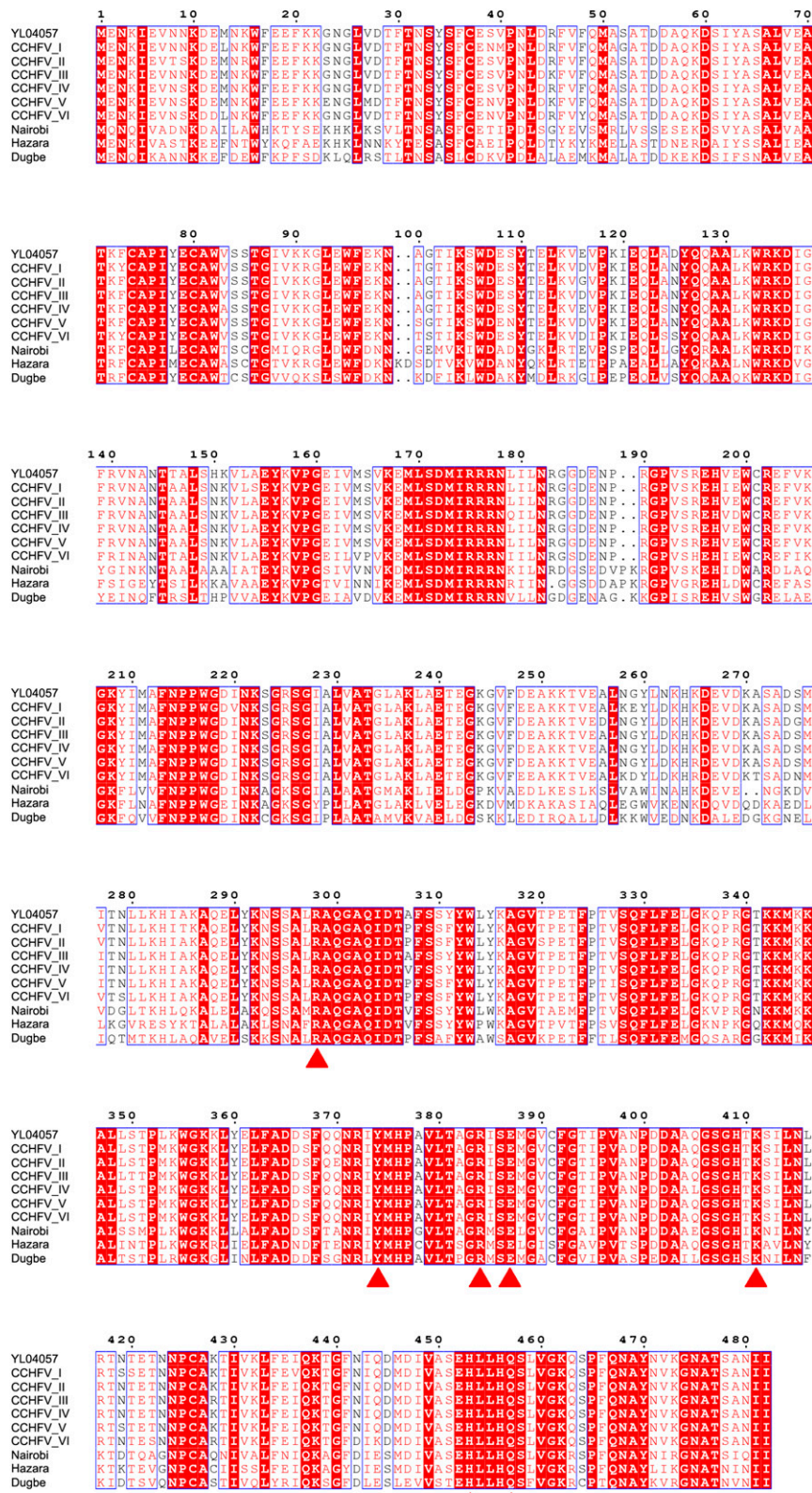


**Fig. S8.** Primary sequence alignment of members of the *Nairovirus* genus. Sequence alignment abbreviations are as follows: YL04057, CCHFV strain YL04057 used in this work; CCHFV\_I, CCHFV subgroup I, strain ArD8194; CCHFV\_II, CCHFV subgroup II, strain UG3010; CCHFV\_III, CCHFV subgroup III, strain ArD39554; CCHFV\_IV, CCHFV subgroup IV, strain Matin; CCHFV\_V, CCHFV subgroup V, strain Drosdov; CCHFV\_VI, CCHFV subgroup VI, strain AP92; Nairobi, Nairobi sheep disease virus strain 6233; Hazara, Hazara virus; Dugbe, Dugbe virus. Residues potentially responsible for endonuclease activity are highlighted by red triangles.

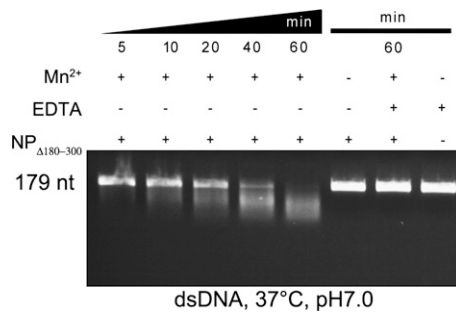


**Fig. S9.** CCHFV NP head domain degrades dsDNA in vitro in the presence of Mn<sup>2+</sup>. CCHFV NP head domain (NP<sub>Δ180-300</sub>) was expressed and purified for in vitro endonuclease assay. Time series of in vitro dsDNA (λ-DNA) degradation assay products are shown. The reaction products of 0.3-μM purified CCHFV NP<sub>Δ180-300</sub> with 100 ng/μL dsDNA substrate at 37 °C are shown after 5, 10, 20, 40, and 60 min. The reaction products were loaded onto a 1.5% agarose gel and stained with ethidium bromide.

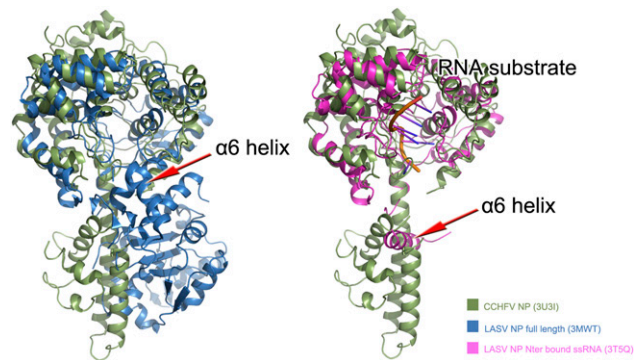


**Fig. S10.** Structural shift of RNA-binding sites in LASV NP and CCHFV NP. (Left) CCHFV NP and full-length LASV NP (PDB code: 3MWT) are superimposed through their N-terminal domains and colored green and blue, respectively. (Right) CCHFV NP is superimposed with the RNA-bound LASV NP N-terminal domain (PDB code: 3T5Q) and colored green and pink. The α6 helix of LASV NP involved in the open gate mechanism is indicated by an arrow.

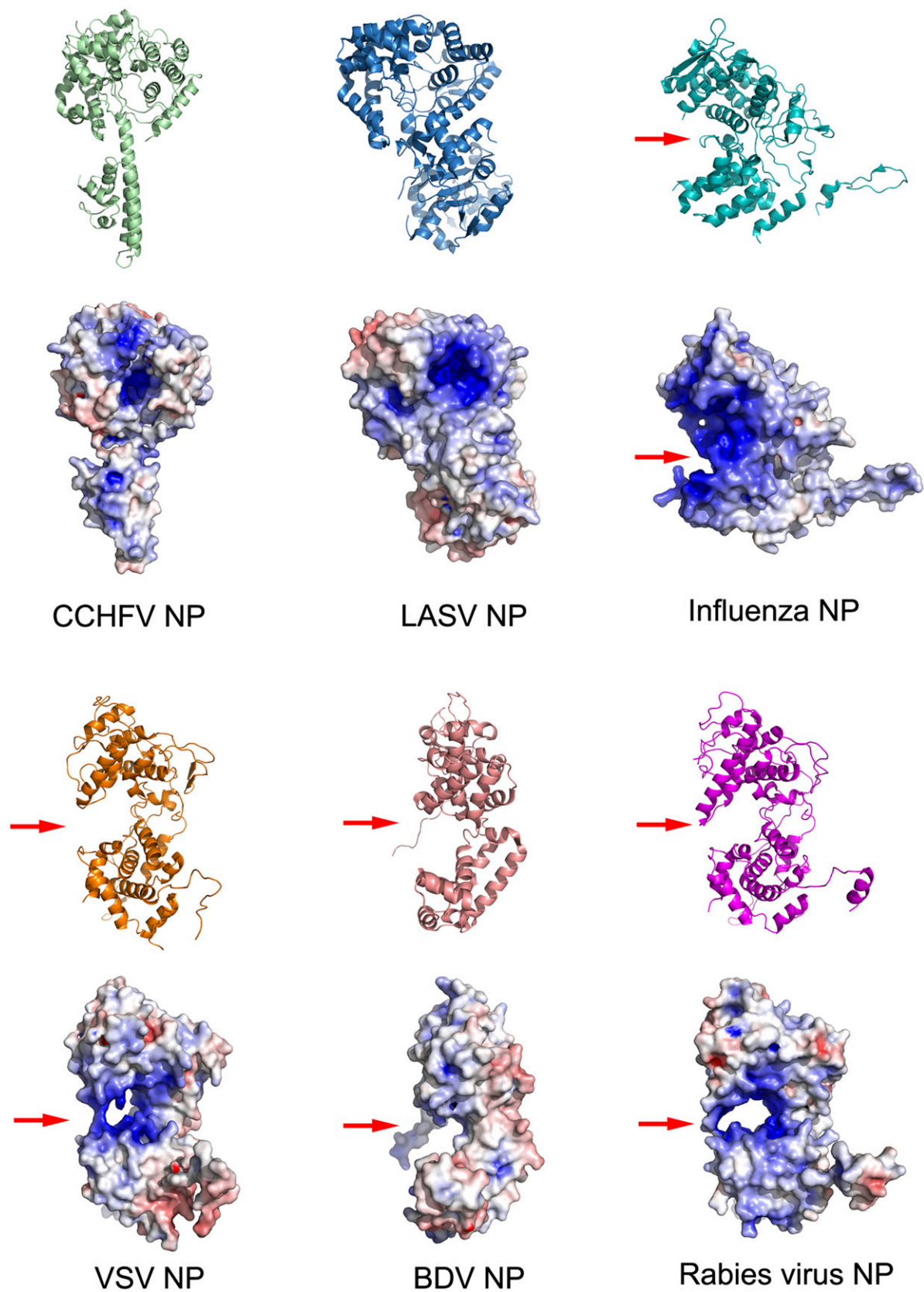


**Fig. S11.** Structural comparison of NPs from (-)ssRNA viruses. The crystal structure of nucleoproteins from CCHFV, LASV (PDB code: 3MTW), influenza virus (PDB code: 2IQH), vesicular stomatitis virus (VSV) (PDB code: 3PTO), borna disease virus (BDV) (PDB code: 1N93), and rabies virus (PDB code: 2GTT) are shown as ribbon and potential surface representations. Positively charged pockets for RNA binding are highlighted with red arrows.